ACS APPLIED MATERIALS & INTERFACES

www.acsami.org

Research Article

# Cancer Cell-Sticky Hydrogels to Target the Cell Membrane of Invading Glioblastomas

Junghwa Cha and Pilnam Kim*

Cite This: *ACS Appl. Mater. Interfaces* 2021, 13, 31371−31378

Read Online

ACCESS | Metrics & More | Article Recommendations | Supporting Information

**ABSTRACT:** Owing to their remarkable infiltrative traits, glioblastomas develop unclear tumor margins toward the brain, hampering the complete resection. Since the remaining invasive cells tend to have resistance to therapeutics and cause recurrence around the surgical voids, this has been a major challenge for glioblastoma treatment. Thus, we design a cancer cell-sticky hydrogel (CSH) that interacts with the glioblastoma cells to impede their invasive motility by modifying the cell membrane with active thiol-enriched interfaces. Highly reactive thiols at the cell surface can make the infiltrated cancer cells adhere to the hydrogel, resulting in increased cell adhesion and decreased motility. Cotreatment with the CSH and chemical inhibitors of the major proinvasive molecules, focal adhesion kinase and hyaluronic acid synthase, maximized the invasion-inhibitory effect. In addition, a significant decrease in tumor mass was achieved via CSH implantation in mouse models. Overall, our results highlight the use of the CSH to inhibit the aggressive invasion as a novel therapeutic strategy against glioblastoma.

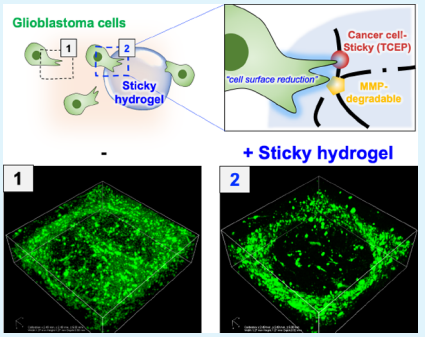


**KEYWORDS:** *postsurgical filling materials, cancer cell-sticky hydrogel, anti-invasion treatment, brain tumor, glioblastoma invasion, cell membrane modification*

## INTRODUCTION

As the outermost cell-extracellular interface, the cell membrane allows the cell to sense and respond to various stimuli from the surrounding microenvironment.[1] Starting from cell receptors at the membrane, the signal cascade triggers the changes of cellular phenotypes, such as adhesion, migration, or proliferation, which is critical in the process of development and healthy tissue homeostasis.[2,3] Therefore, modifying and regulating the "in-and-out" signal and molecules at the cell membrane can be an effective strategy to govern the cellular phenotypes.

One of the representative strategies to take advantage of the modifying cell membrane is treating the tumor cells with specific antibodies to perturb tumor-associated antigens.[4] Since cell surface receptors actively transduce and activate protumorous intracellular signals and interact with the extracellular matrix (ECM) to proceed their invasive motility,[5] the antibody-based treatment can reduce cancer cell motility/proliferation or induce programmed cell death in cancer.[6] Thanks to the technical advances in drug delivery and cell surface engineering, the efficacy and targetability of these soluble biomolecules have been improved; however, there still have been limitations: low therapeutic efficiency and inevitable drug resistance. Moreover, this makes it difficult to find the therapeutic target for the cancer cells that already develop alternative pathways to escape from therapies.

Finding ways to overcome these limitations are critical when treating malignant tumors,[7] especially in case of glioblastoma. Since glioblastoma is a highly infiltrative brain tumor making unclear tumor margins,[8,9] invaded glioblastoma cells preclude complete surgical resection of the entire tumor mass. The infiltrative cells easily lead to development of resistance to adjuvant chemo-/radiotherapy.[10,11] Advanced strategies have been developed to target remaining glioblastoma cells and increase the prognosis of glioblastoma patients:[12,13] antibody-based targeted therapy and polymer-based direct drug delivery such as Gliadel wafers to cure the remaining cells.[14,15] Unfortunately, high interstitial fluid pressure makes it difficult to expect effective delivery and prolonged effect of released drugs at the tumor-resected area.[16,17] Therefore, an alternative therapeutic strategy is urgently needed for effective treatment for glioblastoma patients.

We here propose a cancer cell-sticky hydrogel (CSH) as a new strategy utilizing cell−biomaterial interaction to modify the cell membrane for glioblastoma treatment. By making use of the remarkable infiltrative features, we let the cells interact and invade into the CSH, which can modify the cell membrane into a highly reactive surface, consequently inhibiting further cell spreading. Our previous study introduced a free thiol-

Received: January 7, 2021
Accepted: May 2, 2021
Published: July 1, 2021

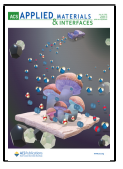

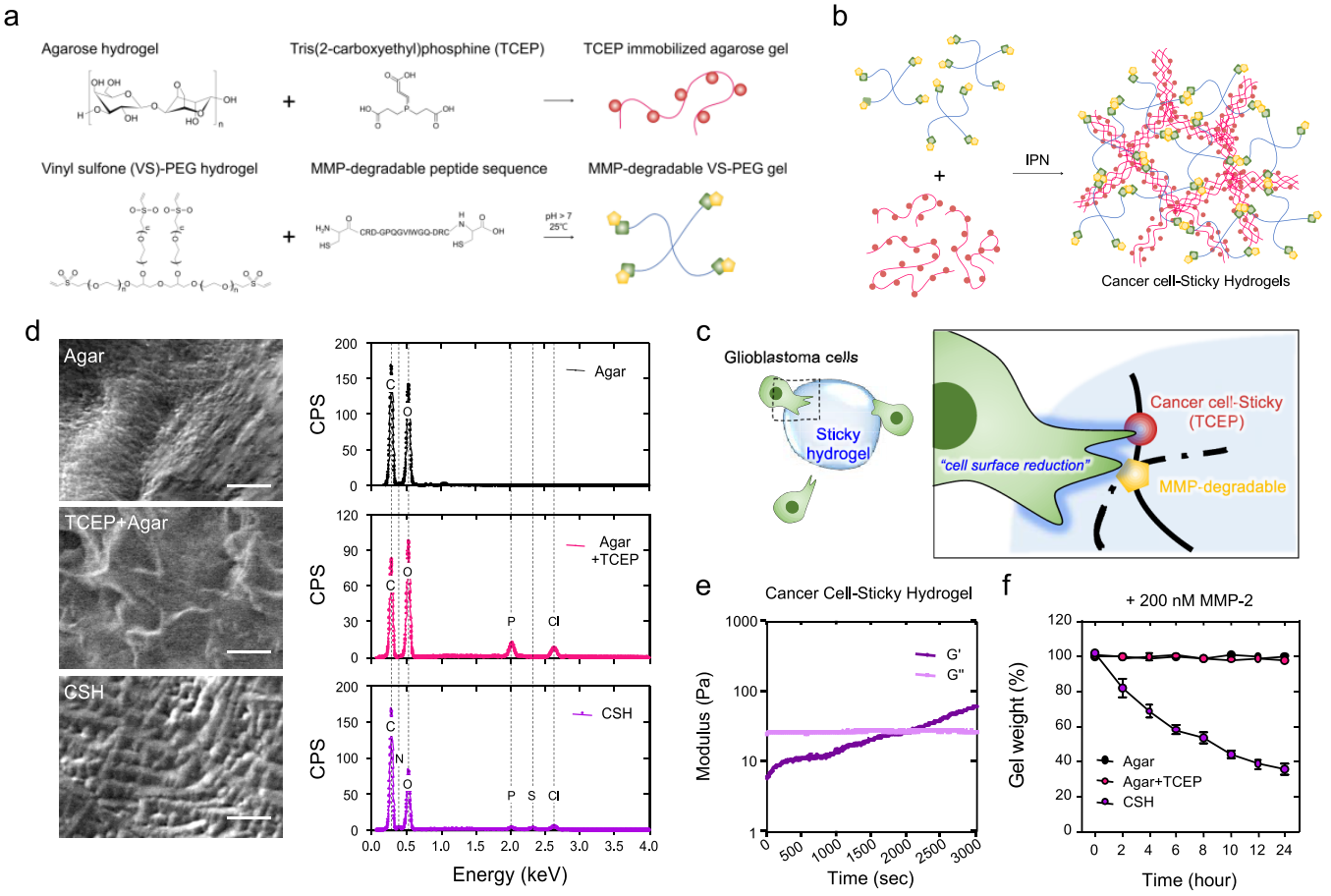


**Figure 1.** Formulation of the CSH. (a) Composition of the CSH: TCEP-immobilized agarose gels and MMP-degradable VS-PEG gels. The agarose hydrogel was selected to immobilize the TCEP reagent. For cell−hydrogel interactions, VS-PEG was modified to be degradable by MMP. (b) Interpenetration of the TCEP-immobilized agarose gel and MMP-degradable VS-PEG gels to form the CSH under physiologic conditions. (c) Schematic illustration of the interface between glioblastoma cell−CSH interaction. (d) Detection of chemical components in the CSH by environmental scanning electron microscopy (E-SEM) with EDS. Scale bar: 10 $\mu$m. (e) Time-variant measurement of isothermic cross-linking of the CSH with storage ($G'$) and loss ($G''$) moduli. (f) Characterization of MMP degradability for the CSH. Hydrogels were mostly stable in the absence of enzyme activity but degraded in response to treatment with MMP-2.

mediated enhanced cell adhesion, which is based on the regulation of oxidoreduction at cell surfaces using tris(2-carboxyethyl) phosphine (TCEP).[18] By reducing the naturally present disulfide bonds on cell surfaces into free thiols, the membranes of glioblastoma cells become highly reactive (adhesive) to the ECM, enabling cell entrapment and further inhibiting tumor motility. To accomplish this working mechanism, we stably immobilized TCEP to make glioblastoma cells expose the free thiols at their cell surfaces. Using the CSH, we observed its effect on modulating the morphology and intracellular signaling. In addition, we fabricated CSH microdroplets (mCSHs) for easy injection and evaluated their effects on trapping glioblastoma cells, resulting in decreased invasion and proliferation with both in vitro 3D radial invasion and in vivo xenograft models.

## RESULTS AND DISCUSSION

We designed a CSH to let the glioblastoma cells interact with and make their membrane highly adhesive. The CSH was fabricated as interpenetrating polymer networks (IPNs) of matrix metalloprotease (MMP)-degradable polyethylene glycol (PEG)-based hydrogels and TCEP-containing agarose hydrogels (Figure 1a,b). The agarose hydrogel was utilized for immobilizing TCEP molecules. Since soluble TCEP can induce cytotoxicity at high concentrations, the TCEP molecules were immobilized within the agarose hydrogel to prevent nonspecific reduction of normal cells by diffusion. In addition, the other components of the CSH were designed to be degradable by MMP. Given that glioblastoma cells mainly express excessive MMP to remodel the ECM during invasion,[19] we utilized MMP-sensitive PEG-based hydrogels to enhance specific targeting of glioblastoma cells. Thus, vinyl sulfone-based PEG (PEG-VS), which is incorporated with MMP-sensitive peptides, was selected as a candidate material that can be easily cross-linked by thermal incubation. The IPN of the MMP-degradable PEG-VS hydrogels and agarose hydrogels immobilized with TCEP was used as a CSH under physiological conditions (Figure 1b). Therefore, CSH components enable the glioblastoma cells to interact and degrade the gels, while stimulating cells to release free thiols and thus causing entrapment thereof (Figure 1c).

Next, energy-dispersive X-ray spectroscopy (EDS) was used to confirm the presence of TCEP and MMP-degradable components in the hydrogel (Figure 1d). Scanning electron microscopy (SEM) coupled with an EDS system can be used to (semi-)qualitatively determine the elementary composition of hydrogel samples based on X-ray emissions. The EDS data revealed the presence of TCEP-immobilized agarose gels and


https://doi.org/10.1021/acsami.1c00388
ACS Appl. Mater. Interfaces 2021, 13, 31371−31378

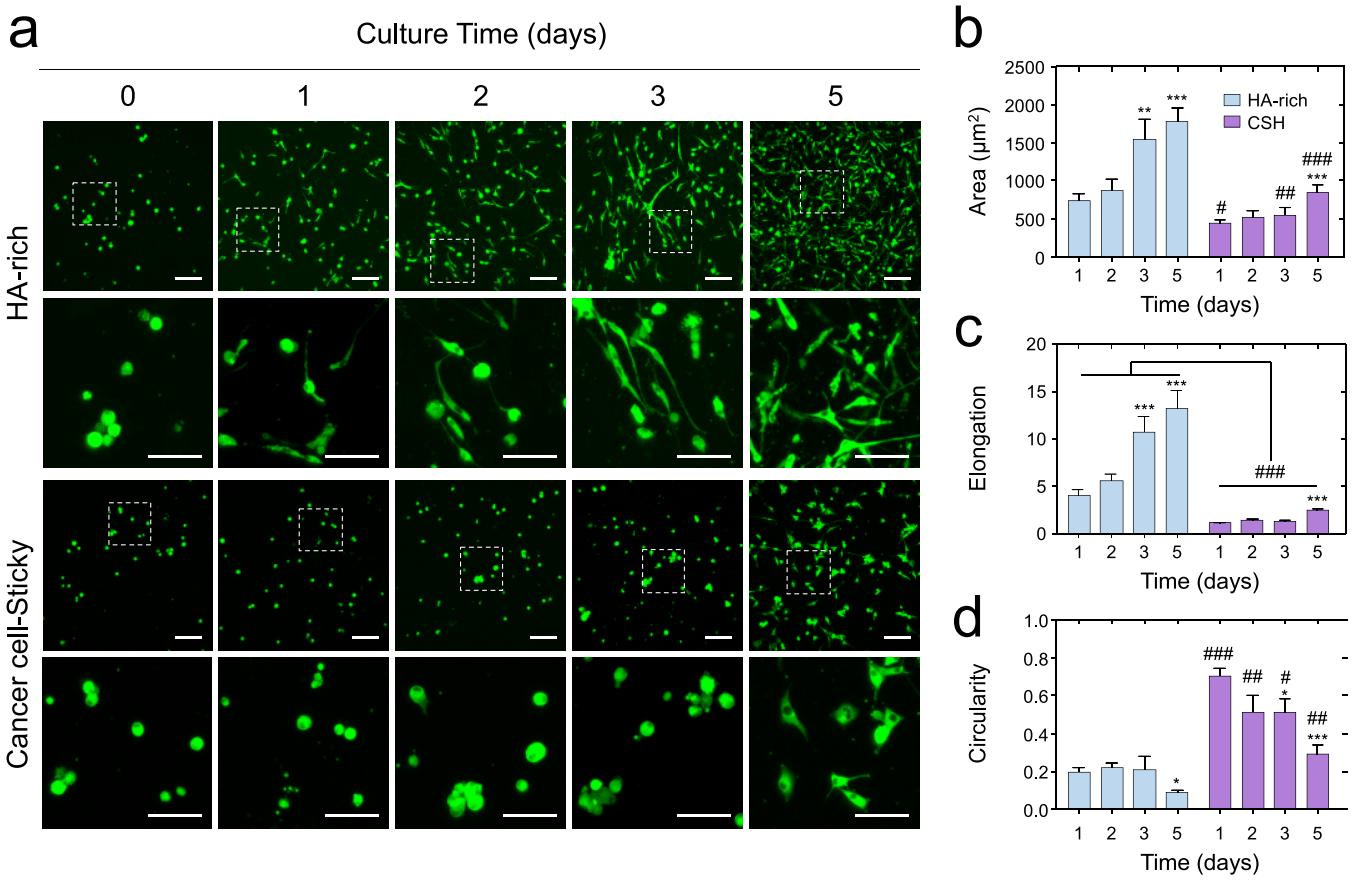


**Figure 2.** Effects of the CSH on cellular morphology and motility of glioblastoma cells. (a) Morphological changes of U87 cells cultivated within the CSH and HA-rich matrix over time. Scale bar: 100 $\mu$m. The HA-rich matrix is the major glioblastoma invasion-promoting extracellular environment. Parametric characterization of (b) cell area, (c) cellular elongation, and (d) cellular circularity within the HA-rich matrix and CSH after 5 days of cultivation. Statistical significance by one-way ANOVA: $^{**}p < 0.01$ and $^{***}p < 0.0001$ for within-group comparisons. $\#p < 0.05$, $\#\#p < 0.01$, and $\#\#\#p < 0.0001$ for between-group comparisons.

two elements, phosphorus (P) and chlorine (Cl), after the addition of the TCEP reagent to the agarose hydrogel, even after interpenetration with the MMP-degradable PEG gels. To confirm that the CSH was cross-linked to form stable gels, we analyzed the gelation kinetics over time under isothermal conditions (Figure 1e). The modulus data of the CSH measured under a time-sweep mode revealed a storage and loss moduli ($G'/G''$) crossover point indicating that the gelation time of the analyzed hydrogels was around 30−35 min after gelation induction. The gelation kinetics of the agarose hydrogel and the TCEP-immobilized agarose hydrogel were similar to that of the CSH (Figure S1).

We also characterized the degradability of the CSH in response to MMP treatment (Figure 1f). The MMP-degradable peptide sequence used here is highly sensitive to MMP-2;[20] we therefore treated the gels with 200 n*m* MMP-2. Both agarose hydrogels (agar) and the TCEP-immobilized agarose hydrogel (agar + TCEP) were mostly stable, even in the presence of enzyme activity, but the CSH was immediately degraded in response to treatment with various concentrations (0, 2, 20, and 200 n*m*) of MMP-2 (Figure S2). The weights of degraded PEG gels decreased in response to MMP-2 treatment. As expected, the degradation of PEG gels was highly dependent on the MMP-2 concentration.

Next, U87 cells were seeded within the CSH to confirm the effects of the CSH on making the tumor cells stick to the hydrogels. A hyaluronic acid (HA)-rich matrix was used to replicate the cell phenotype within a proinvasive microenvironment, as described previously.[21] Within the HA-rich matrix, U87 cells gradually elongated over time, while the cells cultivated within the CSH maintained a relatively round shape (Figure 2a). Quantitative evaluation of the morphology revealed significant differences between cells cultured within the HA-rich matrix and those within the CSH; cells within the CSH exhibited less spreading (Figure 2b−d). Observation of the U87 cells over time revealed that those cultured within the HA-rich environment actively moved within the matrix, while the cells within the CSH rarely moved (Figure S3a).

We next analyzed the ability of the CSH to modulate the phenotype of glioblastoma cells. After 24 h cultivation within the CSH (see Figure S3b), we visualized the free thiols induced in the cell membrane and enhanced adhesion to the gels was visualized by staining with Mal-Alexa Fluor 488 and anti-vinculin antibodies. Within the CSH, the cells expressed more localized vinculin molecules with highly exposed free thiols compared to those in the HA-rich matrix, which maintained a rounded shape with a shrunken cytoskeleton. To examine the effect of TCEP within the CSH, we next cultivated the cells within agarose hydrogels with or without TCEP (Figure S4a). We observed shrunken cytoskeletal structures within the TCEP-containing agarose gels but not within the agarose gels without TCEP. When we fabricated the CSH without TCEP, the cells exhibited an elongated morphology, indicating limited induction of free thiols within


https://doi.org/10.1021/acsami.1c00388
ACS Appl. Mater. Interfaces 2021, 13, 31371−31378

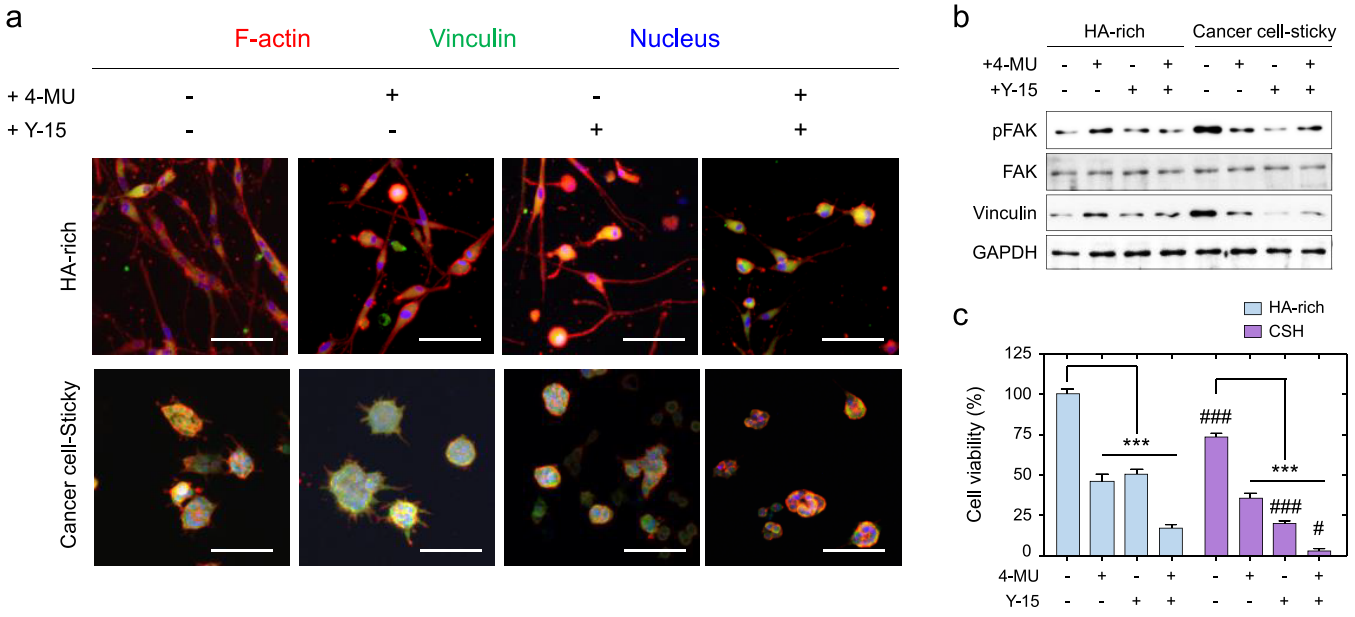


**Figure 3.** Effect of the CSH on modulating the cell membrane of glioblastoma cells. (a) Representative immunofluorescence images of U87 cells within the HA-rich matrix and CSH combined with Y-15 and 4-MU treatment. The images were taken after 5 days of cultivation. (b) Immunoblotting results for FAK, phosphorylated FAK, and vinculin relative to the expression of GAPDH on soluble lysates under each condition. (c) Quantitative measurement of cell viability within the HA-rich matrix and CSH after 5 days of culture. Statistical significance by one-way ANOVA: ***$p < 0.0001$ for within-group comparisons. #$p < 0.05$ and ###$p < 0.0001$ for between-group comparisons.

the gel (Figure S4b). Based on these results, we suggest that the CSH can modify the cell surface to induce abundant free thiols, resulting in preventing cell spreading within the CSH.

We further explore the use of the CSH to inhibit invasiveness to investigate whether the combination of the CSH and chemical drug treatment could enhance efficacy through synergistic effects. We used a hyaluronic acid synthase (HAS) inhibitor (4-MU) and a focal adhesion kinase (FAK) inhibitor (Y-15) to inhibit invasiveness. Since the mesenchymal type of glioblastoma invasion is mediated by proinvasive signaling molecules, both FAK and HAS are involves in facilitating their invasion.[21−24] To observe the inhibitory effects, we treated the U87 cells with 4-MU and Y-15, with 1 mM and 10 $\mu$M of concentration, respectively, for 5 days (Figure S4c). Compared to cells cultured within the HA-rich matrix, cells within the CSH exhibited increased vinculin expression. Under treatment with 4-MU, the cells within both the HA-rich matrix and CSH exhibited increased vinculin expressions (Figure 3a, see Figure S5 for split channel images). These results were confirmed by western blot analysis (Figure 3b). Based on cell viability (Figure 3c), treatment of cells within the CSH with chemical inhibitors of major proinvasive molecules had significant effects on cell viability, suggesting that the efficacy of CSH−chemotherapy cotreatment can be synergistically enhanced.

Next, we fabricated mCSHs to test interaction with invading glioblastoma cells in in vitro and in vivo systems (Figure S6). Using the water−oil emulsion system, we controlled the parameters, such as needle gauge, flow rate, and gel concentration, which can influence the size of the fabricated microdroplets (Figure S6b−d). For parameter optimization, we infused oil flowing at a rate of 0.01 mL/min with the CSH via 30-gauge needles, a flow rate of 0.05 mL/min. We fixed the concentration of MMP-degradable PEG and varied the concentration of the TCEP-containing agarose hydrogel under the above experimental conditions. We obtained uniformly sized (100 $\mu$m) mCSHs using 0.1% TCEP-immobilized agarose hydrogels but not with higher concentrations (Figure S6e−g). The results confirmed that mCSHs can be easily injected using a syringe (Figure S6a).

Next, we tested the effect of mCSHs using a 3D radial invasion assay. To mimic the process of postsurgical invasion, glioblastoma cells were seeded in parenchymal ECM-like hydrogels and hollow centers were filled with tumorous ECM hydrogels (Figure S7a). mCSHs were mixed with the HA-rich hydrogels to verify their cell-trapping effect (Figure 4a). Using the 3D-reconstructed confocal scanning images, the 3D invasions were presented in perspective and top-down views (Figure 4b). Without the mCSHs, U87 cells actively invaded HA-rich gels, filling into the center part. In contrast, with the addition of mCSHs, few U87 cells were invaded within the HA-rich gels, even though HA promotes glioblastoma invasiveness. The invasion was quantified according to the filled area in the center by invading cells. Fewer invasive U87 cells were observed in the mCSH-containing group compared to the control group (Figure 4c). Interestingly, in the presence of mCSHs, the cells exhibited a round shape. This was consistent with our previous observations that cells within the CSH had a shrunken morphology and round shape with induction of free thiols at the cell surfaces. Based on these results, we concluded that the addition of mCSHs to the proinvasive glioblastoma microenvironment can reduce cell motility and alter the cellular phenotype.

To further investigate the therapeutic effects of mCSHs, we cotreated mCSHs and the chemotherapeutic inhibitors, Y-15 and 4-MU, in 3D radial invasion assay. For the mCSH-treating groups, we encapsulated mCSHs within a cell-free area and let the cells invade from peripheral spaces. Compared to the nontreated group, the group treated with triple combination therapy (Y-15 + 4-MU + mCSHs) exhibited remarkably decreased glioblastoma invasion and proliferation (Figure 4d). In addition, compared to the group treated with chemo-


https://doi.org/10.1021/acsami.1c00388
ACS Appl. Mater. Interfaces 2021, 13, 31371−31378

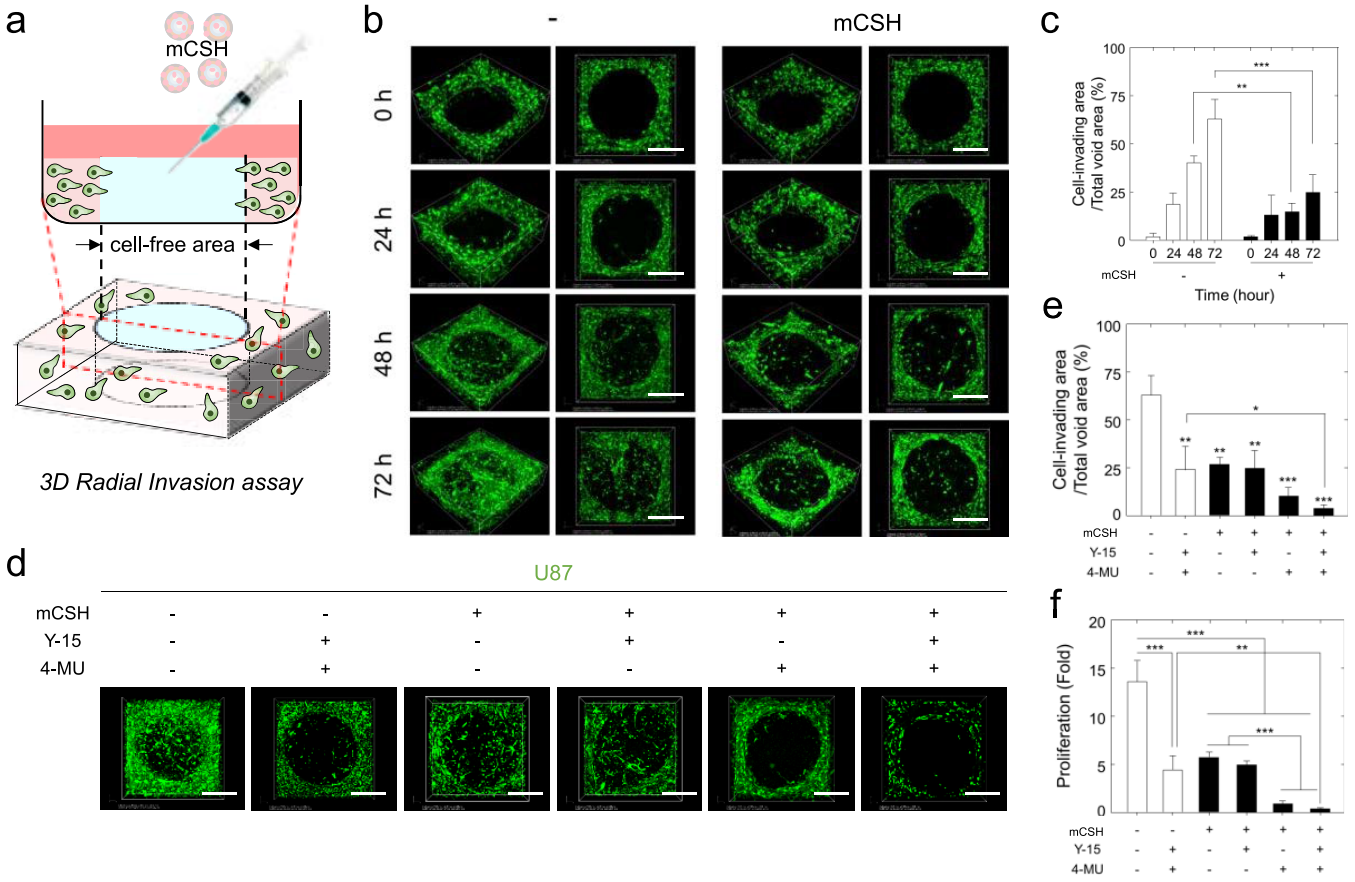


**Figure 4.** Cancer cell-sticky effects of mCSHs in a 3D radial invasion assay. (a) Schematic illustration of 3D radial invasion assay, which consist of parenchymal ECM hydrogels with hollow centers and tumorous ECM for postinvasion analysis. Cross-sectional configuration of the models. (b) Time-course observation of U87 cell invasion into the cell-free void under mCSH-free or mCSH-filled conditions. (c) Quantification of cell-invaded area relative to the total void area in the mCSH-containing group. (d) Cotreatment of mCSHs and chemical inhibitors targeting the major proinvasive molecules, FAK and HAS. Y-15: FAK inhibitor. 4-MU: HAS inhibitor. Scale bar: 200 $\mu$m. (e) Quantification of the cell-invaded area relative to the total void area for the inhibitor cotreatment group. (f) Graph comparing cell viability among the conditions. $^{**}p < 0.01$ and $^{***}p < 0.0001$ by Student's *t*-test.

therapeutics only (Y-15 + 4-MU), fewer remaining cells were observed in the group treated with triple combination therapy. Simultaneous treatment with mCSHs and chemotherapeutics resulted in a remarkable decrease of glioblastoma invasion (Figure 4e). Moreover, this combination therapy also influenced cell proliferation (Figure 4f).

From these results, we suggest that the combination chemotherapy with the CSH may have the synergistic effect to significantly decrease further invasion and proliferation of infiltrated glioblastoma cells.

Lastly, we examined the effect of the CSH in vivo. First of all, to confirm harmful effects of mCSHs itself, we injected mCSHs into normal mouse brains. We showed that there were no adverse effects to mouse survival or tumorigenic effects on the mouse brain (Figure 5a). Next, to evaluate the cancer cell-sticky effect of the mCSHs, we prepared glioblastoma mouse xenograft models. The mCSH-treated mouse brain exhibited weaker bioluminescence signals than the nontreated group, showing longer survival than nontreated mouse glioblastoma models (Figure 5b). In the absence of immobilizing TCEP into the agarose hydrogel, we detected the bioluminescence signals from mouse brains (Figure 5c). We further investigated the effects of cotreatment with mCSHs and chemical inhibitors. Bioluminescence signals from the mCSH-treated mouse brain were rarely detected under treatment with both Y-15 and 4-MU (Figure 5d). Overall, these in vivo data demonstrated the benefit of cancer cell-sticky gels for reducing the survival and invasive characteristics of glioblastoma in mouse models.

## CONCLUSIONS

In the present study, we developed a CSH by engineering cell–biomaterial interfaces that can immobilize the mobility of glioblastoma cells. To meet the major challenges associated with treating glioblastoma patients, a new therapeutic material was designed to target invading tumor cells through cancer cell-specific properties. Reducing the naturally occurring disulfide bonds on tumor cell surfaces facilitates free thiol-mediated adhesion to the CSH, which in turn enables entrapment of residual invading tumor cells within the surgical margin. Therefore, we concluded that the CSH is a promising, novel anti-invasion strategy when administered with chemotherapeutics after brain tumor surgery, effectively inhibiting both invasion and proliferation. The concepts of the CSH could be further developed by incorporating functional modifications and nanomedicines, to modulate cell behavior and may be applicable to other fields, including scaffold-mediated immune therapy.



https://doi.org/10.1021/acsami.1c00388
ACS Appl. Mater. Interfaces 2021, 13, 31371–31378

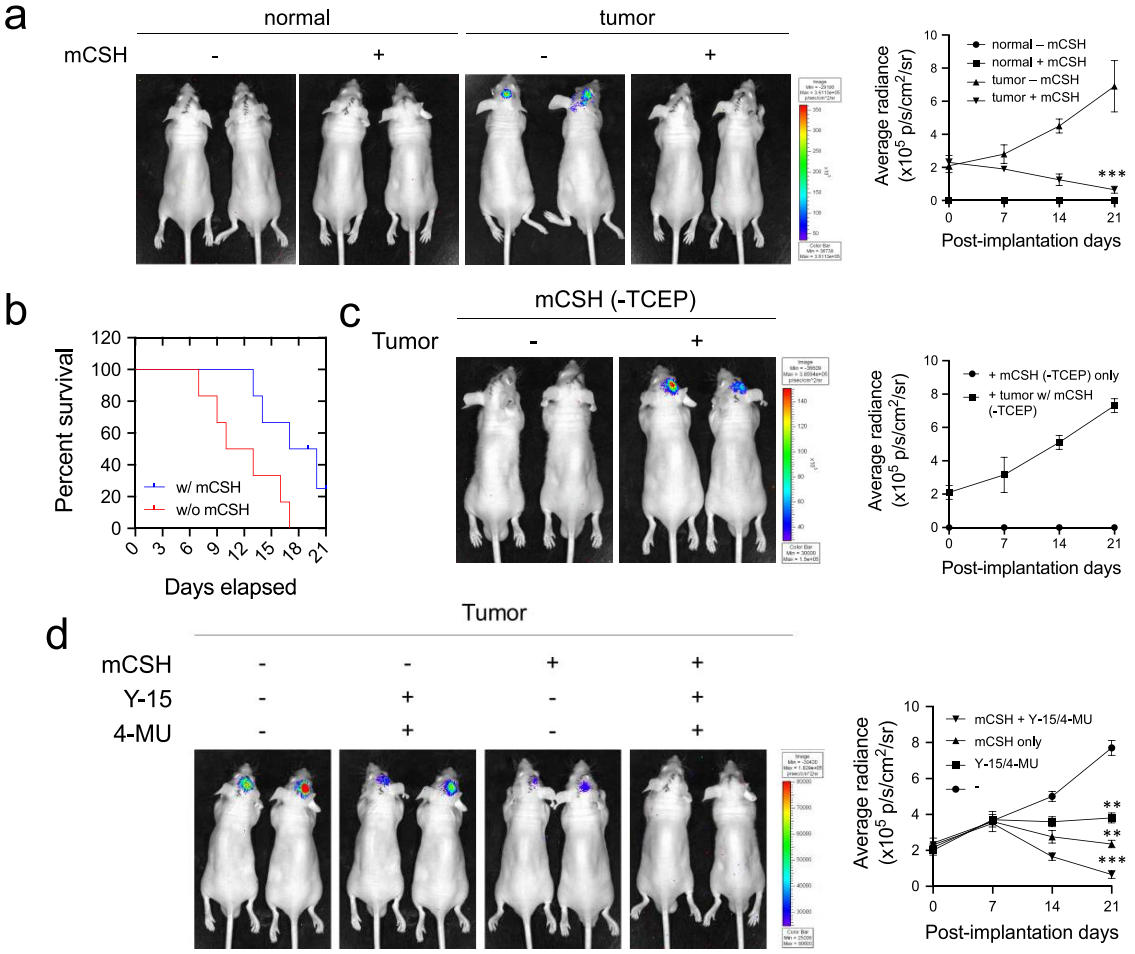


**Figure 5.** Combined therapeutic effect of CSH entrapment and chemotherapy for the glioblastoma mouse xenograft model. (a) Bioluminescence images and signal quantification of the normal and GBM mouse models with and without treatment of mCSHs. (b) Percent survival graph for the glioblastoma mouse xenograft model with (blue) or without (red) treatment of mCSHs. (c) Bioluminescence images and signal quantification for glioblastoma mouse xenograft models under treatment of mCSHs without the reducing effect of TCEP. (d) Bioluminescence images and signal quantification for glioblastoma mouse xenograft models, treated with mCSHs and chemical inhibitors. $^{**}p < 0.01$ and $^{***}p < 0.0001$ by Student's *t*-test.

## METHODS AND MATERIALS

**Preparation of the HA-Rich Matrix and CSH.** To replicate the invasion of glioblastoma cells, U87 glioblastoma cells were cultured within HA-rich ECM hydrogels to recreate the proinvasive environment of brain tumor tissues, as described previously.[21] Briefly, collagen stock was diluted in 4.0 mg/mL collagen solution in sodium hyaluronate (1.01−1.8 MDa, Lifecore Biomedical, Chaska, MN, USA). Then, 1 M NaOH was added to adjust the pH to 7.4 for cell culture. Solutions were mixed thoroughly prior to hydrogel gelation and incubated at 37 °C for 1 h prior to the addition of a superlayer of the cell culture medium.

For redox-regulation, the chemical compound TCEP (Sigma-Aldrich, St. Louis, MO, USA) was used as a reducing agent. To immobilize TCEP, we used low gelling temperature agarose gels (Sigma-Aldrich). The TCEP-containing agarose hydrogel at various concentrations was prepared by boiling agarose powder supplemented with TCEP powder at the desired concentration. MMP-degradable PEG and CSH VS-functionalized 4-arm PEG were purchased from Jenkem Technology (Plano, TX, USA). As a biodegradable motif, an MMP-2-sensitive peptide sequence (Ac-GCRD-GPQGIWGQDRCG; Peptron, Daejeon, Korea) was synthesized and purified. MMP-sensitive PEG hydrogels (10 w/v% concentration) were fabricated through Michael-type addition of thiol-containing peptide sequences, as described previously.[25] We mixed the 3 mM TCEP-containing 0.1 w/v% agarose hydrogel and 10 w/v% MMP-degradable PEG hydrogels at room temperature prior to incubation at 37 °C, to create an IPN (i.e., the CSH).

**Microfabrication of Tumor-Sticky Filling Gels.** The CSH in an aqueous phase (a low-viscosity fluorocarbon oil; HFE7500; Novec; 3 M, Singapore) was used as an oil phase loaded with a 2 wt % surfactant (008-FluoroSurfactant; Ran Biotechnology, Beverly, USA). Both the aqueous and oil phase solutions were infused into Tygon tubes using a syringe pump at different flow rates. For thermal cross-linking, the emulsified gels were incubated at 37 °C for 30 min. Finally, the mCSHs created in HFE7500 were released by adding 1*H*,1*H*,2*H*,2*H*-perfluoro-1-octanol (Sigma-Aldrich), washed with Dulbecco's Modified Eagle's Medium (DMEM; Welgene, Seoul, Korea), and centrifuged to ensure complete oil removal.

**Characterization of CSH Degradability.** To evaluate the MMP-degradable characteristics of PEG components, the weight changes in PEG gels in response to MMP-2 treatment were monitored over 24 h. In addition, FITC-labeled 70 kDa dextran was mixed with the precursor solution of PEG gels to evaluate the release kinetics of the degradation products. Under various concentrations of MMP-2, the release kinetics of dextran from the materials were obtained by monitoring the fluorescence signal.

**Cell Culture.** The human glioblastoma cell line U87MG was used. To enable observation of morphological changes, U87MG was stably transfected with a green fluorescent protein (GFP). U87MG and U87MG-GFP were maintained at 37 °C in an atmosphere of 5% $CO_2$ and 95% air in DMEM (Welgene) supplemented with 10% fetal


https://doi.org/10.1021/acsami.1c00388
ACS Appl. Mater. Interfaces 2021, 13, 31371−31378

bovine serum (Welgene) and 1% penicillin/streptomycin (Welgene). For the experiments, a confluent monolayer of glioblastoma cells was passaged every 3 to 5 days (1:5 ratio).

**Cell Labeling with Maleimide-Alexa Fluor 488.** U87 glioblastoma cells were reduced with the TCEP (Sigma-Aldrich) reducing agent for 30 min and washed twice with phosphate-buffered saline (PBS). After elimination of the reducing solution, Maleimide-Alexa Fluor 488 C5 (Mal-Alexa Fluor 488; 1 mg/mL, Thermo Fisher, Waltham, MA, USA) dissolved in PBS at a final concentration of 3 $\mu$g/mL was added to the cells and incubated for 20 min at 37 °C. After incubation, the Mal-Alexa Fluor 488-labeled, TCEP-treated U87 cells were washed with PBS and fixed with 4% paraformaldehyde solution for 20 min. To visualize nuclei, samples were dyed with DAPI (Sigma-Aldrich). For further observation, fluorescence signals were visualized using a confocal microscope (Nikon, Tokyo, Japan).

**Immunocytochemistry.** U87 glioblastoma cells were fixed in 4% paraformaldehyde and permeabilized with 0.5% Triton X-100. After blocking with 1% bovine serum albumin (BSA)-PBS, the cells were incubated with anti-vinculin antibodies (Abcam, Cambridge, UK). For counterstaining, nuclei were stained for 15 min using 2 mg/L DAPI (Sigma-Aldrich). Samples were washed with PBS between steps to reduce the background prior to examination by confocal microscopy.

**3D Radial Invasion Assay.** To verify the anti-glioblastoma invasion effect, the mCSHs were introduced into a 3D radial invasion assay. To construct this model, a polydimethylsiloxane (PDMS) blocker was used to create a cell-free region at the center. Collagen hydrogels containing U87 cells were gelated around the PDMS blocker. After 24 h incubation, the PDMS blocker was removed and the HA-rich hydrogels containing mCSHs were injected into the cell-free region. Invasion of fully confluent U87 cells toward the HA-rich ECM gels with or without mCSHs was evaluated for 72 h.

**Establishment of the In Vivo Glioblastoma Xenograft Model.** All animal experimental procedures were performed by the approval of the Animal Care Committee of KAIST (KA2018−62) ($n$ = 6). In addition, the authors conducted all animal experiments in accordance with the ethical protocol given by the Korean Ministry of Health and Welfare. Male athymic Balb/c nude mice (Samtako, Osan, Korea) aged 7 to 8 weeks were used as xenograft models. Mice with similar weight were randomly divided as control and experimental groups. Luciferase-transfected U87MG glioblastoma cells (U87-luc) with a density of $1 \times 10^5$ cells in the culture medium were implanted into the right frontal lobe of nude mice within the skull on the stereotaxic frame. U87-luc cells only or U87-luc mixed with mCSHs were injected into the mouse brain using a microinfusion syringe pump (Harvard Apparatus, Holliston, MA, USA) at a speed of 0.1 $\mu$L/min. For studying the combined therapeutic effect of CSH entrapment with chemotherapy, the mice after 7 days were randomized and daily treated with 4-MU with a concentration of 100 mg/kg or Y-15 with a concentration of 10 mg/kg by intraperitoneal administration. At the end-point of the experiment, mice were sacrificed and their brain tissues were fixed with 10% neutral buffered formalin for gross observation.

**Statistical Analysis.** For all experiments, data were collected over three independent experiments. All statistical data were analyzed using GraphPad Prism 8. Data are presented as the mean ± standard error of the mean (SEM). Independent samples were compared using Student's $t$-test. Groups were compared by one-way analysis of variance (ANOVA) followed by Tukey's post hoc test.

## ■ ASSOCIATED CONTENT

### Supporting Information

The Supporting Information is available free of charge at https://pubs.acs.org/doi/10.1021/acsami.1c00388.

Detailed information for the experimental setting and supplementary figures (time-variant measurement of isothermic cross-linking of the agarose hydrogel and TCEP-containing agarose hydrogel, characterization of the CSH degradability in response to treatment with various concentrations of MMP-2, representative fluorescence images to visualize the morphologies of U87 cells cultivated within the HA-rich gels and CSH gels, the effect of TCEP within the agarose gels and CSH gels, production of the microfabricated CSH for easy injection, and the schematic illustration and experimental process of 3D radial invasion assay) (PDF)

## ■ AUTHOR INFORMATION


### Corresponding Author

**Pilnam Kim** − *Department of Bio and Brain Engineering, KAIST, Daejeon 34141, Korea; KAIST Institute for Health Science and Technology, Daejeon 34141, Korea;* orcid.org/0000-0003-0611-6525; Email: pkim@kaist.ac.kr

### Author

**Junghwa Cha** − *Department of Bio and Brain Engineering, KAIST, Daejeon 34141, Korea; KAIST Institute for Health Science and Technology, Daejeon 34141, Korea; Department of Bioengineering, University of California, Berkeley, California 94720, United States*

Complete contact information is available at: https://pubs.acs.org/10.1021/acsami.1c00388


### Author Contributions

J.C. and P.K. conceived and designed the study; J.C. performed the experiments and analyzed the data; and J.C. and P.K discussed the data and wrote the manuscript.

### Notes

The authors declare no competing financial interest.

## ■ ACKNOWLEDGMENTS

This research was supported by the Basic Science Research Program through the National Research Foundation of Korea (NRF) funded by the Ministry of Education (NRF-2019R1A2C2084142) and by a grant of the Korea Health Technology R&D Project through the Korea Health Industry Development Institute (KHIDI), funded by the Ministry of Health and Welfare, Republic of Korea (grant number: HI14C1324). This work was also supported by the KAIST Future Systems Healthcare Project from the Ministry of Science and ICT (KAISTHEALTHCARE42).

## ■ REFERENCES


(1) Miranti, C. K.; Brugge, J. S. Sensing the Environment: A Historical Perspective on Integrin Signal Transduction. *Nat. Cell Biol.* **2002**, *4*, E83−E90.

(2) Bonnans, C.; Chou, J.; Werb, Z. Remodelling the Extracellular Matrix in Development and Disease. *Nat. Rev. Mol. Cell Biol.* **2014**, *15*, 786−801.

(3) Jean, C.; Gravelle, P.; Fournie, J. J.; Laurent, G. Influence of Stress on Extracellular Matrix and Integrin Biology. *Oncogene* **2011**, *30*, 2697−2706.

(4) Gan, H. K.; Van Den Bent, M.; Lassman, A. B.; Reardon, D. A.; Scott, A. M. Antibody-Drug Conjugates in Glioblastoma Therapy: The Right Drugs to the Right Cells. *Nat. Rev. Clin. Oncol.* **2017**, 695.

(5) Quail, D. F.; Joyce, J. A. The Microenvironmental Landscape of Brain Tumors. *Cancer Cell* **2017**, *31*, 326−341.

(6) Pearson, J. R. D.; Regad, T. Targeting Cellular Pathways in Glioblastoma Multiforme. *Signal Transduct. Target. Ther.* **2017**, *2*, 17040.

(7) Hanahan, D.; Weinberg, R. A. Hallmarks of Cancer: The next Generation. *Cell* **2011**, *144*, 646−674.
(8) Huse, J. T.; Holland, E. C. Targeting Brain Cancer: Advances in the Molecular Pathology of Malignant Glioma and Medulloblastoma. *Nat. Rev. Cancer* **2010**, *10*, 319−331.
(9) Bellail, A. C.; Hunter, S. B.; Brat, D. J.; Tan, C.; Van Meir, E. G. Microregional Extracellular Matrix Heterogeneity in Brain Modulates Glioma Cell Invasion. *Int. J. Biochem. Cell Biol.* **2004**, *36*, 1046−1069.
(10) Omuro, A.; DeAngelis, L. M. Glioblastoma and Other Malignant Gliomas: A Clinical Review. *JAMA* **2013**, *310*, 1842−1850.
(11) Stupp, R.; Mason, W. P.; van den Bent, M. J.; Weller, M.; Fisher, B.; Taphoorn, M. J. B.; Belanger, K.; Brandes, A. A.; Marosi, C.; Bogdahn, U.; Curschmann, J.; Janzer, R. C.; Ludwin, S. K.; Gorlia, T.; Allgeier, A.; Lacombe, D.; Cairncross, J. G.; Eisenhauer, E.; Mirimanoff, R. O. Radiotherapy plus Concomitant and Adjuvant Temozolomide for Glioblastoma. *N. Engl. J. Med.* **2005**, *352*, 987−996.
(12) Lesniak, M. S.; Brem, H. Targeted Therapy for Brain Tumours. *Nat. Rev. Drug Discov.* **2004**, *3*, 499−508.
(13) Rich, J. N.; Bigner, D. D. Development of Novel Targeted Therapies in the Treatment of Malignant Glioma. *Nat. Rev. Drug Discov.* **2004**, *3*, 430−446.
(14) Brem, H.; Mahaley, M. S.; Vick, N. A.; Black, K. L.; Schold, S. C.; Burger, P. C.; Friedman, A. H.; Ciric, I. S.; Eller, T. W.; Cozzens, J. W.; Kenealy, J. N. Interstitial Chemotherapy with Drug Polymer Implants for the Treatment of Recurrent Gliomas. *J. Neurosurg.* **1991**, *74*, 441−446.
(15) Perry, J. Gliadel® Wafers in the Treatment of Malignant Glioma: A Systematic Review. *Curr. Oncol.* **2007**, *14*, 189−194.
(16) Pardridge, W. M. The Blood-Brain Barrier: Bottleneck in Brain Drug Development. *NeuroRx* **2005**, *2*, 3−14.
(17) Saraiva, C.; Praça, C.; Ferreira, R.; Santos, T.; Ferreira, L.; Bernardino, L. Nanoparticle-Mediated Brain Drug Delivery: Overcoming Blood-Brain Barrier to Treat Neurodegenerative Diseases. *J. Control. Release* **2016**, *235*, 34−47.
(18) Cha, J.; Kim, H.; Hwang, N. S.; Kim, P. Mild Reduction of the Cancer Cell Surface as an Anti-Invasion Treatment. *ACS Appl. Mater. Interfaces* **2018**, *10*, 35676−35680.
(19) Wang, M.; Wang, T.; Liu, S.; Yoshida, D.; Teramoto, A. The Expression of Matrix Metalloproteinase-2 and -9 in Human Gliomas of Different Pathological Grades. *Brain Tumor Pathol.* **2003**, *20*, 65−72.
(20) Patterson, J.; Hubbell, J. A. Enhanced Proteolytic Degradation of Molecularly Engineered PEG Hydrogels in Response to MMP-1 and MMP-2. *Biomaterials* **2010**, *31*, 7836−7845.
(21) Cha, J.; Kang, S. G.; Kim, P. Strategies of Mesenchymal Invasion of Patient-Derived Brain Tumors: Microenvironmental Adaptation. *Sci. Rep.* **2016**, *6*, No. 24912.
(22) Cha, J.; Koh, I.; Choi, Y.; Lee, J.; Choi, C.; Kim, P. Tapered Microtract Array Platform for Antimigratory Drug Screening of Human Glioblastoma Multiforme. *Adv. Healthc. Mater.* **2015**, *4*, 405−411.
(23) Golubovskaya, V. M.; Huang, G.; Ho, B.; Yemma, M.; Morrison, C. D.; Lee, J.; Eliceiri, B. P.; Cance, W. G. Pharmacologic Blockade of FAK Autophosphorylation Decreases Human Glioblastoma Tumor Growth and Synergizes with Temozolomide. *Mol. Cancer Ther.* **2013**, *12*, 162−172.
(24) Kim, Y.; Kumar, S. CD44-Mediated Adhesion to Hyaluronic Acid Contributes to Mechanosensing and Invasive Motility. *Mol. Cancer Res.* **2014**, *12*, 1416−1429.
(25) Lutolf, M. P.; Hubbell, J. A. Synthesis and Physicochemical Characterization of End-Linked Poly(Ethylene Glycol)-Co-Peptide Hydrogels Formed by Michael-Type Addition. *Biomacromolecules* **2003**, *4*, 713−722.


https://doi.org/10.1021/acsami.1c00388
*ACS Appl. Mater. Interfaces* 2021, 13, 31371−31378